

Detection of blood-brain barrier dysfunction using advanced imaging methods to predict seizures in dogs with meningoencephalitis of unknown origin

Erez Hanael¹  | Shelly Baruch¹ | Orit Chai¹ | Zohar Nir¹ | Kira Rapoport¹ | Marco Ruggeri¹  | Itzhak Eizenberg¹ | Dana Peery¹ | Alon Friedman^{2,3} | Merav H. Shamir¹ 

¹Hebrew University Koret School of Veterinary Medicine-Veterinary Teaching Hospital, Rehovot, Israel

²Departments of Physiology and Cell Biology, Brain, and Cognitive Sciences, Zlotowski Center for Neuroscience, Ben-Gurion University of the Negev, Beer Sheva, Israel

³Department of Medical Neuroscience, Faculty of Medicine, Dalhousie University, Halifax, NS, Canada

Correspondence

Merav H. Shamir, Koret School of Veterinary Medicine, The Hebrew University of Jerusalem, P.O. Box 12, Rehovot 67100, Israel.
 Email: merav.shamir@mail.huji.ac.il

Funding information

Israeli Science Foundation (ISF), Grant/Award Number: 717-15

Abstract

Background: The blood-brain barrier (BBB), which separates the intravascular and neuropil compartments, characterizes the vascular bed of the brain and is essential for its proper function. Recent advances in imaging techniques have driven the development of methods for quantitative assessment of BBB permeability.

Hypothesis/Objectives: Permeability of the BBB can be assessed quantitatively in dogs with meningoencephalitis of unknown origin (MUO) and its status is associated with the occurrence of seizures.

Animals: Forty dogs with MUO and 12 dogs without MUO.

Methods: Retrospective, prospective cohort study. Both dynamic contrast enhancement (DCE) and subtraction enhancement analysis (SEA) methods were used to evaluate of BBB permeability in affected (DCE, $n = 8$; SEA, $n = 32$) and control dogs (DCE, $n = 6$; SEA, $n = 6$). Association between BBB dysfunction (BBBD) score and clinical characteristics was examined. In brain regions where BBBD was identified by DCE or SEA magnetic resonance imaging (MRI) analysis, immunofluorescent staining for albumin, glial fibrillary acidic protein, ionized calcium binding adaptor molecule, and phosphorylated moths against decapentaplegic homolog 2 were performed to detect albumin extravasation, reactive astrocytes, activated microglia, and transforming growth factor beta signaling, respectively.

Results: Dogs with BBBD had significantly higher seizure prevalence (72% vs 19%; $P = .01$) when compared to MUO dogs with no BBBD. The addition of SEA to routine MRI evaluation increased the identification rate of brain pathology in dogs with MUO from 50% to 72%.

Conclusions and Clinical Importance: Imaging-based assessment of BBB integrity has the potential to predict risk of seizures in dogs with MUO.

Abbreviations: BBB, blood-brain barrier; BBBD, blood-brain barrier dysfunction; CNS, central nervous system; CSF, cerebrospinal fluid; DCE, dynamic contrast enhanced; GFAP, glial fibrillary acidic protein; iba1, ionized calcium binding adaptor molecule; MRI, magnetic resonance imaging; MUO, meningoencephalitis of unknown origin; pSMAD2, phosphorylated moths against decapentaplegic homolog 2; SEA, subtraction enhancement analysis; TGF- β , transforming growth factor beta

This is an open access article under the terms of the Creative Commons Attribution-NonCommercial-NoDerivs License, which permits use and distribution in any medium, provided the original work is properly cited, the use is non-commercial and no modifications or adaptations are made.

© 2022 The Authors. *Journal of Veterinary Internal Medicine* published by Wiley Periodicals LLC on behalf of American College of Veterinary Internal Medicine.

KEYWORDS

blood-brain barrier, epilepsy, meningoencephalitis

1 | INTRODUCTION

Meningoencephalitis of unknown origin (MUO) is a group of idiopathic, noninfectious, central nervous system (CNS) inflammatory diseases in which a definitive histopathological diagnosis is lacking.¹ Granulomatous meningoencephalitis, necrotizing meningoencephalomyelitis, and necrotizing leukoencephalitis are 3 distinct MUO disorders identified by histological evaluation.²⁻⁴ Although the pathogenesis of MUO is unclear, it is most likely multifactorial, combining genetic predisposition with factors triggering an excessive immunologic response.^{3,4} Tentative diagnosis is based on clinical presentation, inflammatory cerebrospinal fluid (CSF) findings, magnetic resonance imaging (MRI) abnormalities, and lack of an identified infectious agent.^{3,5} Although MRI is an important diagnostic test, a lesion is detected in 48% to 96%^{6,7} of cases and results rarely are correlated with the severity of disease.^{6,7} Identifying and treating MUO is still a challenge. The survival rate of diagnosed and treated dogs is 90% in the first month and only 60% at 1-year follow-up.⁶ Seizures occur in >20% of MUO dogs and are associated with poorer prognosis.^{6,8} Nevertheless, no diagnostic test can predict seizures or poor outcome in dogs with MUO.

Blood-brain barrier dysfunction (BBBD) has been implicated in the pathophysiology of several neurological pathologies including inflammatory, degenerative, and vascular diseases, as well as in propagation and maintenance of seizures and epilepsy.⁹⁻¹¹ Leakage and brain exposure to albumin was shown to initiate transcriptional modulation of genes related to the inflammatory transforming growth factor beta (TGF- β) signaling pathway. Increased TGF- β signaling results in activation of astrocytes, degradation of the extracellular matrix, decreased inhibitory synaptic transmission, and generation of new excitatory synapses in both experimental settings and in clinical cases in humans and dogs with seizures.¹²⁻¹⁷

Recently established MRI analysis algorithms allow evaluation and quantification of BBBD in experimental animals and as part of the clinical evaluation in humans and dogs.¹⁸⁻²³ Two of these techniques are dynamic contrast-enhanced MRI (DCE-MRI) and subtraction enhancement analysis (SEA).^{18,19} The DCE-MRI algorithm identifies brain voxels with BBBD by a positive slope of contrast accumulation over time. Subtraction enhancement analysis is a less demanding quantitative method that detects permeable voxels by comparing intensity between precontrast and postcontrast scans in relation to a predetermined reference tissue threshold.¹⁹ In both methods, the overall scores of BBBD are given as percentage of permeable voxels in the entire brain.

We implemented 2 imaging methods to assess BBBD in dogs with MUO and its association with clinical findings and occurrence of seizures. Tissues obtained at necropsy from dogs that died from the diseases were used to colocalize imaging-based evidence for BBBD with immunofluorescence for albumin leakage and TGF- β signaling.

2 | MATERIAL AND METHODS

Clinical and imaging data used in our study were part of the clinical evaluation except for DCE-MRI, which was done in addition to the routine MRI sequences. The addition of the dynamic sequences was approved by the Hebrew University Veterinary Teaching Hospital Ethics Committee (KSVM-VTH/26_2016) and the owners signed an informed consent form. Retrieval of information from the hospital's medical records archive was similarly approved. Dogs that died from their disease were subjected to necropsy and brain extraction after written consent from the owners.

2.1 | Animals and study design

There were 2 study arms (Figure 1) based on the MRI protocol used. The dogs in the DCE-MRI group were included in a prospective study (approved by the Hebrew University Veterinary Teaching Hospital Ethics Committee [KSVM-VTH/26_2016]) assessing BBB integrity in dogs with various neurological diseases. The SEA group included dogs diagnosed with MUO that underwent routine clinical evaluation including MRI. Ours was a retrospective analytical cross-sectional study conducted using archived MRI and medical record data. The MRI records of all dogs admitted to the Koret School of Veterinary of Veterinary Medicine Teaching Hospital (KSVM) between 2014 and 2019 with neurological dysfunction were reviewed. Only dogs diagnosed with MUO were included. Medical history, complete physical and neurological examination findings, CBC, serum biochemical profile, and CSF analysis results were obtained from the medical records. Seizure history, type, frequency, and time from last seizure to imaging also were documented. The control group included 6 dogs that underwent head MRI for evaluation of extracranial diseases.

In both study arms, diagnosis of MUO was based on clinical signs of focal or multifocal lesions, inflammatory CSF findings, and negative antibody titers to common infectious agents. Magnetic resonance imaging abnormalities were evident in some of the dogs and included focal or multifocal hyperintense lesions on T2-weighted sequences with or without T1-weighted sequences postcontrast enhancement.

Dogs that died from the disease during the study period were subjected to necropsy examination and brain extraction, and samples were processed as described below.

2.2 | Quantification of BBBD score

The MRI studies were performed using a 0.35 Tesla magnet (Magnetom C, Siemens Healthineers, Berlin, Germany), whereas dogs

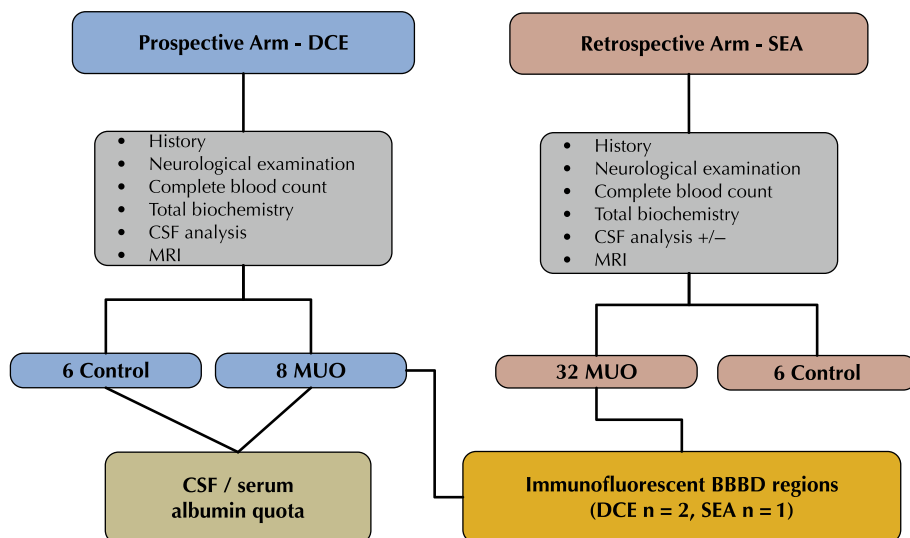


FIGURE 1 Flowchart of the study design showing the 2 arm of the study, namely dynamic contrast enhanced (DCE) and subtraction enhancement analysis (SEA)

were under general anesthesia maintained with 1% to 2% isoflurane and constant oxygen flow (100%, 2 L/h) after intubation.

The DCE-MRI sequences included 7 transverse T1-weighted gradient recalled (GE) sequences, 1 before and 6 immediately after contrast administration (excitation time [TE]: 6.75-7.30 ms, relaxation time [TR]: 192-445 ms, flip angle: 90°, slice thickness: 3.5-4 mm, interslice gap: 3.85-4.40 mm, field of view [FOV]: 13.50 × 13.50 cm – 18 × 18 cm, reconstruction matrix: 192 × 192).

Subtraction enhancement analysis was performed using the following MRI sequences: T1-weighted spin echo (SE) in transverse plane (TE: 21 ms, TR: 642-916 ms, flip angle: 90°, slice thickness: 3.5-4.0 mm, interslice gap: 3.85-4.40 mm, FOV: 13.50 × 13.50 cm – 18 × 18 cm, reconstruction matrix: 256 × 256-384 × 384). The T1-weighted sequences taken before and after the injection of contrast were used for the SEA performed using in-house Matlab scripts (MATLAB 2018b, The MathWorks, Inc., Natick, Massachusetts).

In both study arms, gadolinium-diethylenetriamine pentaacetate (Magnetol) was injected IV at a dosage of 0.3 mL/kg as a bolus.

For BBB evaluation, preprocessing included extracting the entire brain volume by semiautomatic algorithm, in which the user sampled the white and gray matter intensity values in the T1 SE scan. Brain mask was created and extracted automatically by the algorithm. Images then were registered by using in-house Matlab functions to align each postcontrast image to the baseline precontrast image.

The DCE-MRI analysis was done by fitting a linear curve to the dynamic scan intensities of 6 consecutive postcontrast T1-weighted gradient echo scans (T1 gradient co+contrast_1-6). This protocol is a modification of that used in humans and dogs as previously reported.^{18,23} A signal $s(t)$ is fitted to a linear curve such that: $s(t) = A \times t + B$, where the slope (A) is the rate of wash-in or wash-out of the contrast agent from the brain parenchyma.

A BBB permeability map was generated for the entire brain and represented the slope values of each voxel (Figure 2A).

In the SEA, the intensity difference between the precontrast and the postcontrast scan was calculated and presented as a percentage

of the precontrast signal intensity. This value was termed the percentage of intensity difference (PID). The temporal muscle of each dog was used as a reference value, because it represents a tissue with no blood tissue barrier and is subjected to the unique physiological variables of each dog.²³ The mean reference PID value of 2 cm² of the temporal muscle was calculated in each dog. Distribution of PID values of brain voxels of all MUO and control dogs and those of the temporal muscles was aligned (Figure 2B). The PID value distribution curves mostly overlapped and were separated toward the left slope of each curve, representing high PID values. Maximal differences among the 3 curves were detected for PID values above the mean PID of the temporal muscles (Figure 2C). Several thresholds for the determination of permeable voxels were evaluated and the 1 that associated best with seizures was set as the mean PID of the temporal muscle plus 1 SD (Figure 2B; HT).

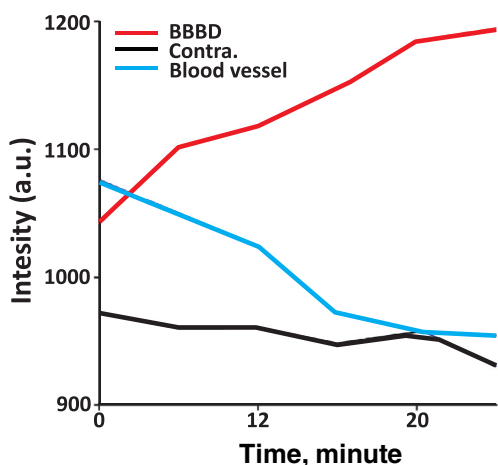
The BBB score was determined for both DCE and SEA in 3 steps. First, all positive brain voxels were detected as described above. Second, a region growing procedure was applied to each positive voxel involving repeatedly connecting neighboring voxels. Small noisy clusters (ie, <4 neighboring voxels) were removed using a morphological filtering procedure. Lastly, a BBB score was assigned to each dog by calculating the percentage of positive voxels in their brain images.

The BBB score similarly was calculated for all control dogs. The upper value for normal BBB score (NBBB) was set at the mean BBB score of control dogs plus 2 SD (mean of 0.33%). All values exceeding this threshold were considered as representing BBBB.

2.3 | Serum and CSF albumin measurements

Albumin and total protein concentrations were measured in the CSF and serum of all dogs included in the prospective DCE-MRI study. Quantification was performed using a wet chemistry auto-analyzer Cobas-6000 (Roche, Rottkreutz, Switzerland) at 37°C.

(A) Dynamic contrast enhanced- MRI (DCE)



(B) Subtraction enhancement analysis (SEA)

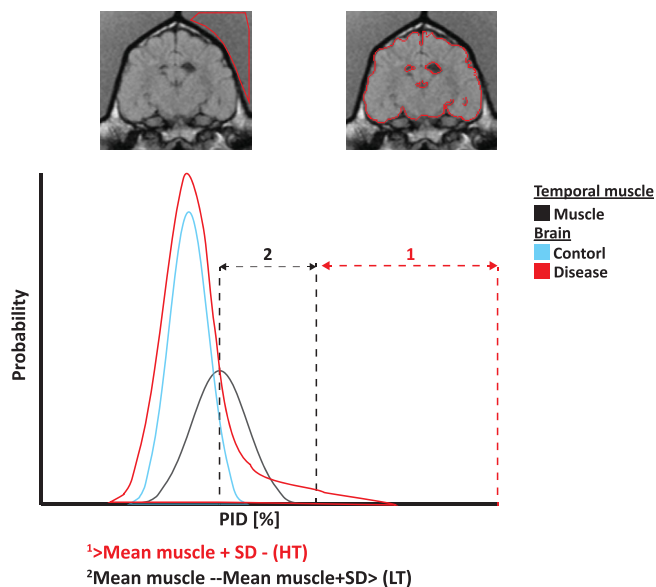


FIGURE 2 Overview of blood-brain barrier (BBB) analysis. A, Dynamic contrast enhanced (DCE) analysis. Graph shows concentration of contrast agent as a function of time (slope) in 3 areas: affected region with BBBD (red), unaffected contralateral area with an intact BBB (Contra., black), and blood vessel (blue). B, Subtraction enhancement analysis (SEA). Top: Region of interest in the temporal muscle and representation of the brain mask. Bottom: Graph of distribution of brain voxel percentage of intensity difference (PID) shows the proportion of positive voxels in each of the calculation methods. Positive enhanced voxels were defined as either above the mean PID of the temporal muscle plus 1 standard deviation (HT, red arrows) or between the mean PID of the temporal muscle and the mean plus 1 standard deviation (LT, black arrows)

2.4 | Immunofluorescence studies

Brains of dogs that were euthanized because of the disease (n = 3) within the first week from diagnosis were removed and immediately

immersed in 4% paraformaldehyde for a week before they were sectioned and embedded in paraffin. Sections of brain regions where BBB dysfunction was detected by either DCE or SEA methods were cut at a thickness of 5 μm, stretched in water at 35°C and mounted on positively charged microscope slides (Denville Scientific, M1021). Slides were subsequently air-dried in an incubator at 37°C overnight and deparaffinized in graded ethanol. One slide from each region underwent hematoxylin and eosin staining for pathology and classification of MUO type. Additional slides were incubated in Tris-EDTA buffer (pH 9.0) at 80°C for 20 minutes for antigen retrieval, and then incubated in 5% donkey serum and 0.1% Triton X-TBS for 1 hour at room temperature and overnight at 4°C with the following antibodies: antiphospho-Smad2 (rabbit, Millipore AB3849-I, 1:200), antidog albumin (Goat, Abcam ab194215, 1:500), anti-ionized calcium binding adaptor molecule (iba1) (rabbit, Abcam ab178847, 1:500), and antigial fibrillary acidic protein (GFAP) (mouse, sigma C9205 cy3 conjugated, 1:500). After washing, slides were incubated for 1 hour at room temperature with the following secondary antibodies: rabbit Alexa Fluor 568, mouse Alexa Fluor 488, and chicken Alexa Fluor 647 (Jackson ImmunoResearch Labs, diluted 1:500). Slide-mounted brain sections were treated with TrueBlack Lipofuscin Autofluorescence Quencher (Biotium #23007) and incubated with 4',6-diamidino-2-phenylindole (900 nM; Sigma-Aldrich). Regions of interest, where BBB permeability maps had a positive slope value, were imaged using an Axio Imager M1 microscope equipped with AxioCam MRm camera (Zeiss, Germany).

2.5 | Data analysis

The MRI analyses were done by an investigator who was blinded to the diagnosis and clinical details. The Shapiro-Wilk test was used to assess distribution of continuous variables. Two-sample *F* tests for equal variances were used for quantitative comparison of variables. To compare quantitative variables between 2 independent groups, the 2-sample *t* test or the nonparametric Mann-Whitney test were used according to the Shapiro-Wilk test results. Receiver operating characteristic (ROC) analysis²⁴ was performed to assess the predictive value of the BBBD score for seizures. All tests were 2-tailed, and *P* ≤ .05 was considered significant. All statistical tests were performed using Matlab scripts (MATLAB 2018b, The MathWorks, Inc., Natick, Massachusetts). Data are presented as median and range.

3 | RESULTS

3.1 | Demographic data

Overall, 52 dog were included in this study. In the prospective DCE arm of the study (n = 14), there were 8 dogs with MUO and 6 healthy control dogs. Among the 8 dogs in the MUO group, 6 were females, median age was 5.5 (range, 5.0-12.0) years, and median body weight

MUE

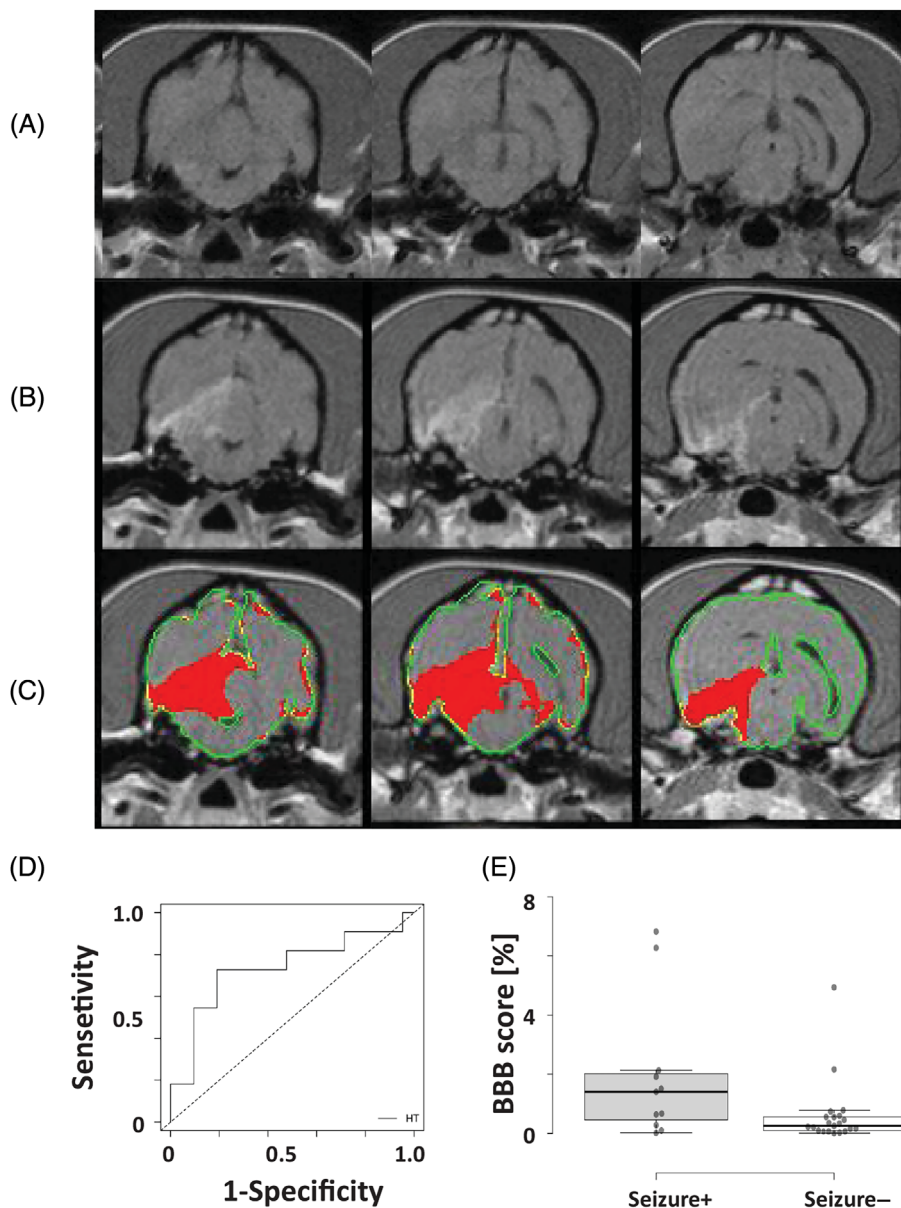


FIGURE 3 Detection of blood-brain barrier dysfunction (BBBD) in dogs with meningoencephalitis of unknown origin (MUO) using subtraction enhancement analysis (SEA). A-C, Representation of MUO in a dog. A, T1-weighted precontrast images; B, T1-weighted postcontrast images; C, positive voxels as detected by SEA using the high threshold (HT, red) were superimposed on postcontrast T1-weighted images. D, Receiver operating characteristic curve (ROC) analysis of BBBD scores was performed to determine the optimal cutoff point between MUO dogs with and without seizures. E, Box plot comparing BBB scores of MUO dogs with or without epileptic seizures. Center lines show the medians; box limits indicate the 25th and 75th percentiles as determined; whiskers extend to 1.5 times the interquartile range from the 25th and 75th percentiles (seizure+; n = 11, seizure-; n = 21)

was 3.9 (range, 1.7-40.0) kg. Seizures were reported in 6/8 MUO dogs.

Among the 6 healthy control dogs, 2 were females, median age was 4.5 (range, 4.5-5.0) years, and median body weight was 20.7 (range, 5.0-30) kg. Cerebrospinal fluid was obtained from all dogs and found to be normal.

In the SEA retrospective arm of the study, there were 32 dogs with MUO, of which 22 were females (68.75%). Median age was 6 (range, 0.7-14.0) years and median body weight was 5.7 (range, 1.8-34.1) kg. Seizures were recorded in 34.4% of the dogs (11/32).

The 6 dogs of the control group underwent MRI and were diagnosed with extracranial diseases, including acute blindness (n = 2), idiopathic vestibular syndrome (n = 2), medial ear infection (n = 1), and general weakness (n = 1). In this group, 1 dog was female, median age

was 7 years (range, 5-10 years), and median body weight was 35.5 kg (range, 2.0-42.0 kg). Cerebrospinal fluid was obtained in 3/6 dogs and found to be normal.

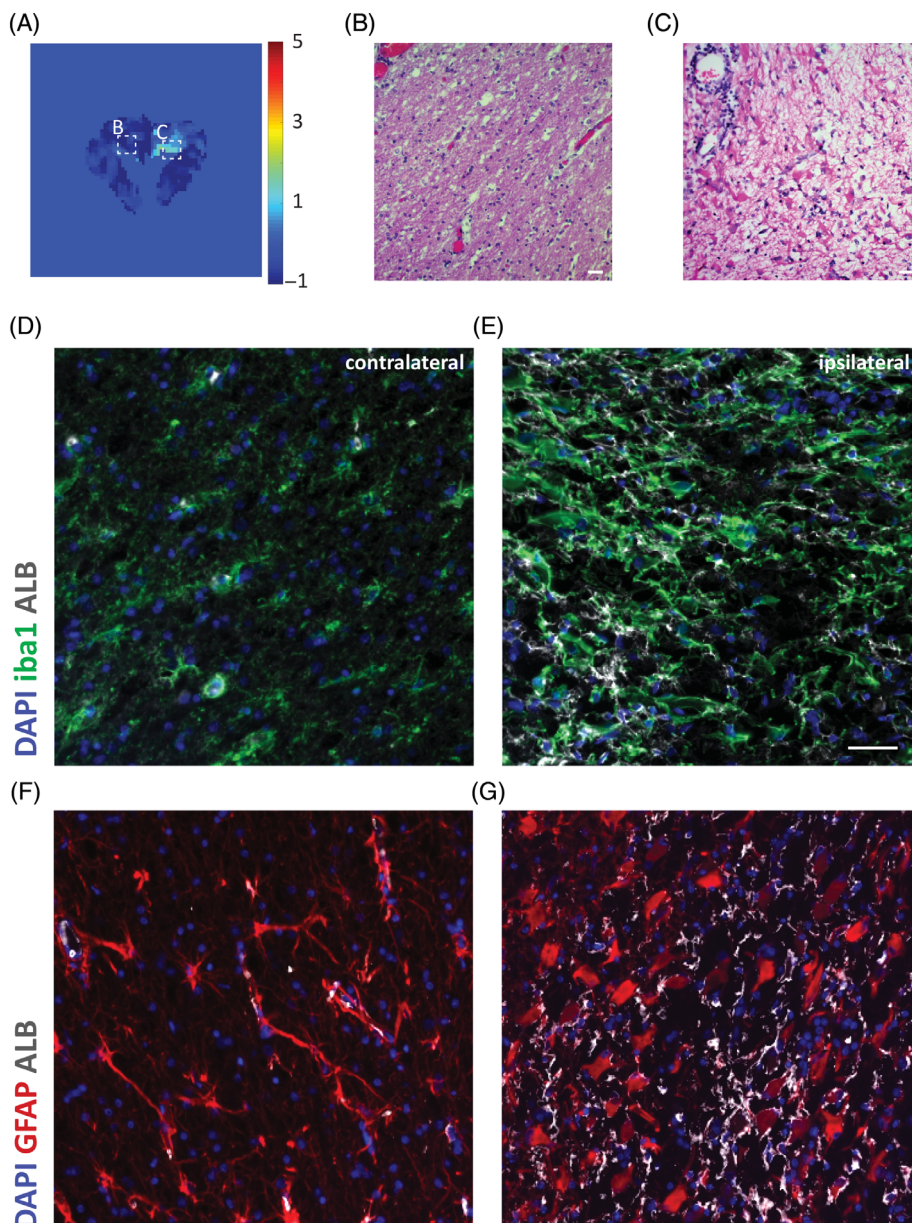
3.2 | BBBD quantification using DCE-MRI

Evaluation of BBB using the DCE-MRI-based method identified a median BBB score of 15.8% (range, 5.0%-69.0%) in the MUO group vs 13.9% (range, 3.1%-25.2%) in the control group.

Based on the threshold, BBBD was detected in 3 of the 8 dogs with MUO.

Dogs with MUO had significantly higher albumin quota (AQ) than dogs in the control group (1.21 [range, 0.50-4.42] vs 0.54 [range, 0.24-0.57]; $P = .02$, Mann-Whitney test).

FIGURE 4 Distinct areas of blood-brain barrier dysfunction (BBBD) in necrotizing leukoencephalomyelitis. A, Image of brain slice acquired by linear dynamic contrast-enhanced magnetic resonance imaging (DCE-MRI) and visualized by color-coded permeability maps, from negative slope values in blue to positive in red. B, Section showing normal white matter contralateral to the BBBD-affected region. B, Hematoxylin and eosin-stained section shows edema and necrosis, with gemistocytic astrogliosis and perivascular lymphocytic cuffing. Original magnification $\times 40$. D-G, Microscope images of coronal sections through the normal contralateral region (D, F) and the ipsilateral BBBD-affected region (F, G) stained for albumin (white), microglia marker iba1 (green) or astrocytic marker glial fibrillary acidic protein (GFAP; red) and DAPI nuclear staining (blue). Increased albumin uptake in the ipsilateral side with BBBD is colocalized with astrocytes and microglia. Scale bars = 20 μm



Dogs with BBBD had higher AQ than dogs with normal BBB (2.07 [range, 1.83-4.42] vs 0.92 [range, 0.50-1.30]; $P = .03$, Mann-Whitney test).

3.3 | BBBD quantification using SEA

Evaluation of routine MRI sequences (T2, FLAIR, T1 \pm contrast) by radiologists identified no brain abnormalities in 50% (16/32) of dogs with MUO. Among the dogs with detected brain abnormalities, T2 and FLAIR hyperintensities were identified in all of them (16/16), T1 hypointensities were identified in 2 and T1 enhancement was identified in 10. In addition, ventricular enlargement was identified in 56.2% (18/32) of all cases (for details, see Supplementary Table S1). Using advanced image analysis, BBBD was identified in 17 of the 32 dogs (53%) when applying the SEA method. In 7 of these 17 dogs, no

abnormalities were identified by routine MRI evaluation. The addition of SEA to routine MRI evaluation increased the identification rate of brain abnormalities from 50% to 72% (23/32) of dogs with MUO (Figure 3A-C). Five dogs that were classified as NBBB had brain abnormalities detected by the radiologists. All 5 dogs had areas of T2 and FLAIR hyperintensities at different locations. In 1 dog, mild postcontrast enhancement was identified in the periventricular and gray and white matter zones (Table 1; Supplementary Information).

3.4 | Immunofluorescence findings in brain regions where BBBD was detected

Brain areas with BBBD as detected using either DCE-MRI ($n = 2$) or SEA ($n = 1$) included the left temporal lobe gray matter and left

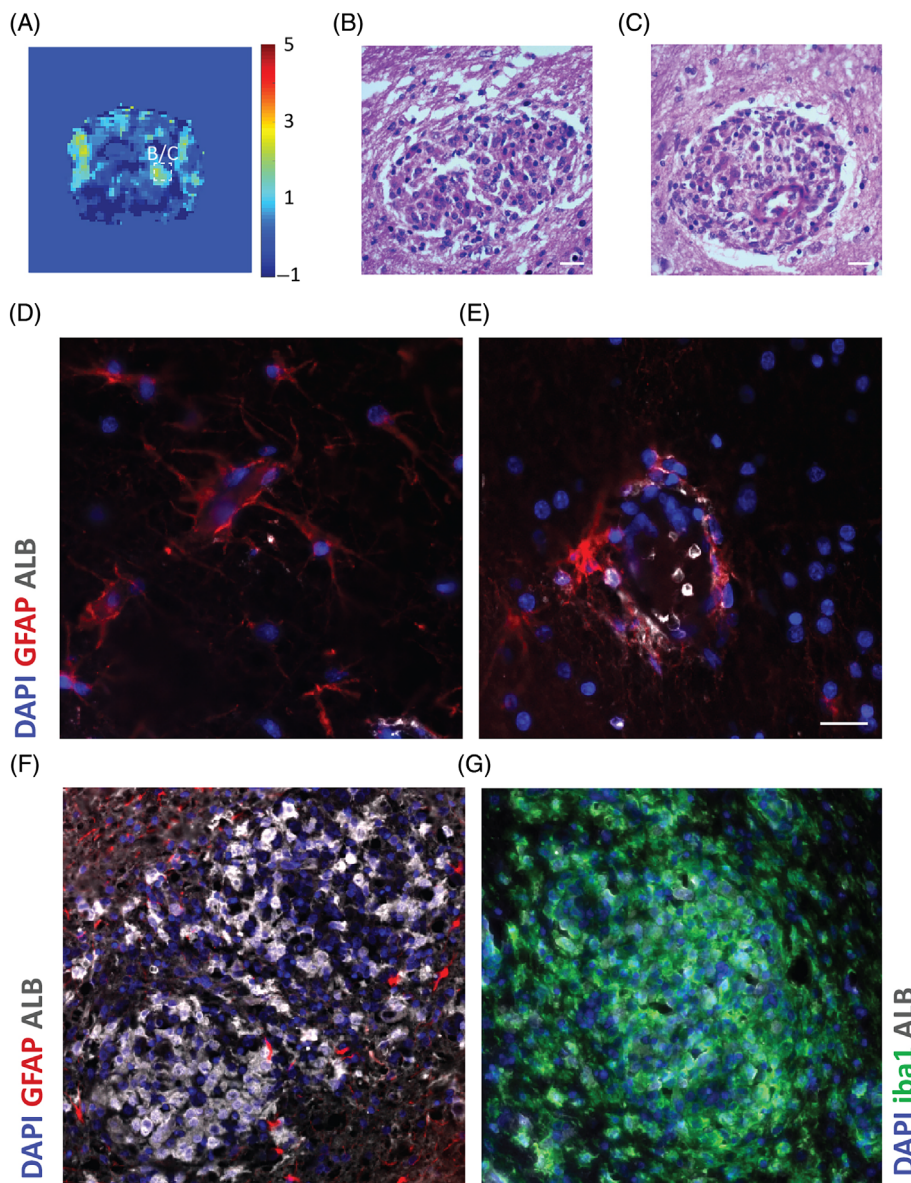


FIGURE 5 Distinct areas of glial fibrillary acidic protein (BBBD) in granulomatous meningoencephalitis. A, Image of a brain slice acquired by linear dynamic contrast-enhanced magnetic resonance imaging (DCE-MRI) and visualized by color-coded permeability maps. B, C, Hematoxylin and eosin-stained sections from regions where BBBD was detected: a characteristic lesion in midbrain parenchyma (B) and a perivascular cuff around a blood vessel comprising a predominantly mononuclear inflammatory cell infiltrate (C). Original magnification $\times 40$. D, E, Microscope images of coronal sections through the midbrain with no lesions. Normal blood vessel from contralateral side (D) and blood vessel with perivascular cuff around it (E) were stained for albumin (white), astrocytic marker glial fibrillary acidic protein (GFAP; red) and DAPI nuclear staining (blue). Albumin uptake is colocalized with astrocyte end feet around the blood vessels. F, G, Microscope images of a lesion in a midbrain region with BBBD stained for albumin (white), astrocytic marker GFAP (red) and DAPI nuclear staining (blue) (F) or for albumin, microglia marker *iba1* (green) and DAPI (G). Severe albumin uptake in the lesion with active astrocytes is colocalized with *iba1*-positive cells. Scale bars = 20 μm

hippocampus (case 1), the right hemisphere white matter of the frontal lobe, dorsal to an enlarged lateral ventricle (case 2) and white matter of the left internal capsule (case 3). These were compared using immunofluorescent assays to brain regions with intact BBB, which included the histologically intact cortex of the temporal lobe adjacent to the lesion (case 1), the contralateral white matter of the frontal lobe (case 2) and the contralateral white matter of the internal capsule (case 3). All BBBD regions had extravasation of albumin colocalized with reactive astrocytes and microglia (Figures 4-6). Similarly, we identified higher albumin in reactive astrocytes colocalized with higher levels of phosphorylated mothers against decapentaplegic homolog 2 (*pSMAD2*) expression within the cytoplasm. These findings suggest activation of TGF- β signaling in these astrocytes by albumin, which was not detected in the contralateral intact BBB brain regions (Figure 7).

3.5 | Association between BBBD and clinical variables

In both the SEA and DCE groups, 50% of the dogs with MUO were identified with BBBD ($n = 20$; 3 and 17 dogs, respectively). No differences were found in age, sex, or weight between dogs with and without BBBD. When BBBD score was calculated using SEA, significantly higher scores were found in MUO dogs presented with seizures than in dogs with no seizures (median of 1.4 [range, 0.02-6.82] vs 0.25 [range, 0.01-4.94]; $P = .03$, Mann-Whitney test). We then performed ROC analysis to define the optimal cutoff of the BBBD score that distinguishes between MUO dogs with and without seizures. The AUC of the BBB score was 0.73 (confidence interval, 0.53-0.94) for the development of seizures. A cutoff of 0.64 showed a sensitivity of 72% and specificity of 85% (Figure 3D).

FIGURE 6 Distinct areas of glial fibrillary acidic protein (BBBD) in necrotizing meningoencephalomyelitis. A, Image of a brain slice acquired by linear subtraction enhancement analysis (SEA) and visualized by color-coded permeability maps, where red signifies positive values above HT. B, C, Hematoxylin and eosin-stained section showing BBBD-affected region with edema, necrosis and intense inflammation with parenchymal histiocytic, microglial infiltrates and perivascular lymphocytic cuffing. Original magnification $\times 40$. D, E, Microscope images of coronal sections through a normal temporal cortex adjacent to the disrupted region. F, G, Microscope images of coronal sections through the region identified with BBBD. Sections were stained for albumin (white), microglia/macrophages marker iba1 (green) or astrocytic marker glial fibrillary acidic protein (GFAP; red) and DAPI nuclear staining (blue). Increased albumin uptake in the ipsilateral side with BBBD is colocalized with astrocytes and microglia. Scale bars = 20 μm

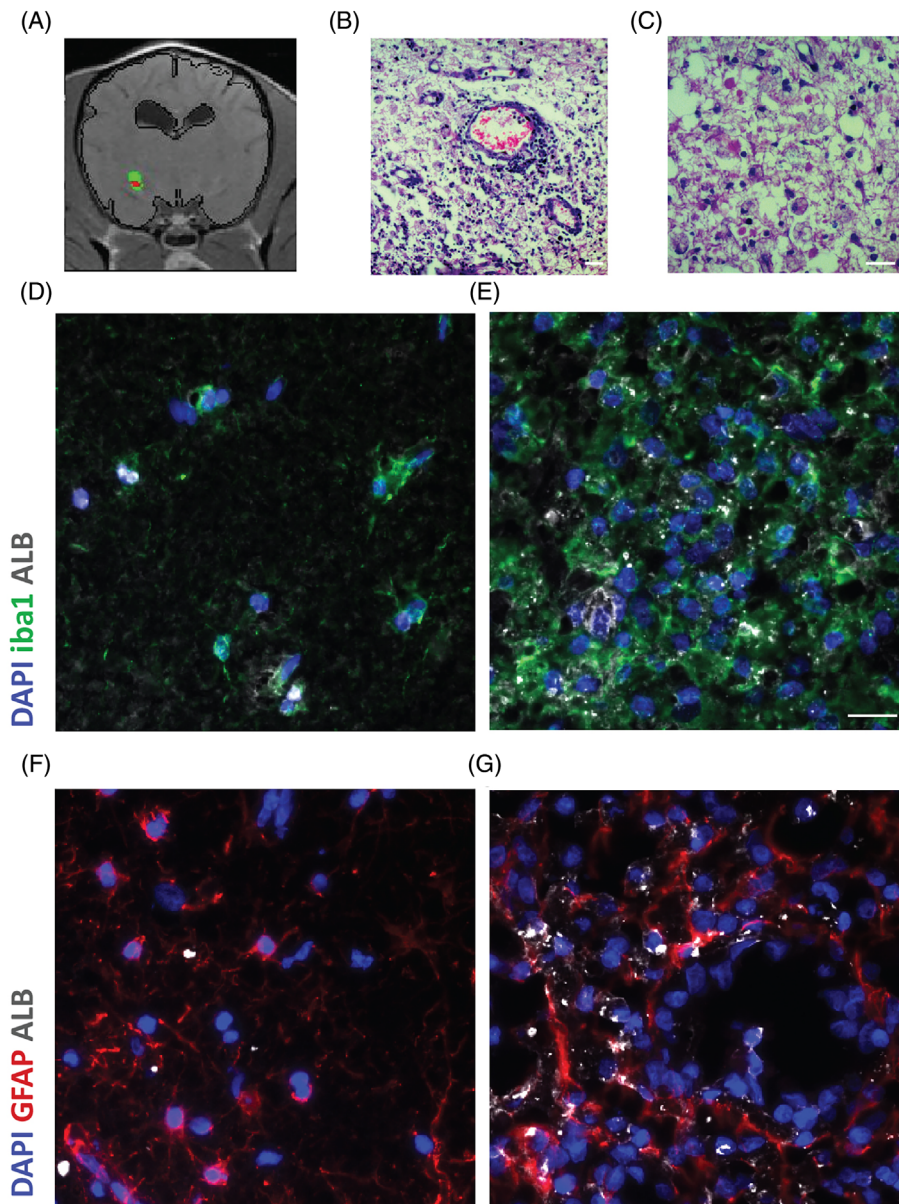
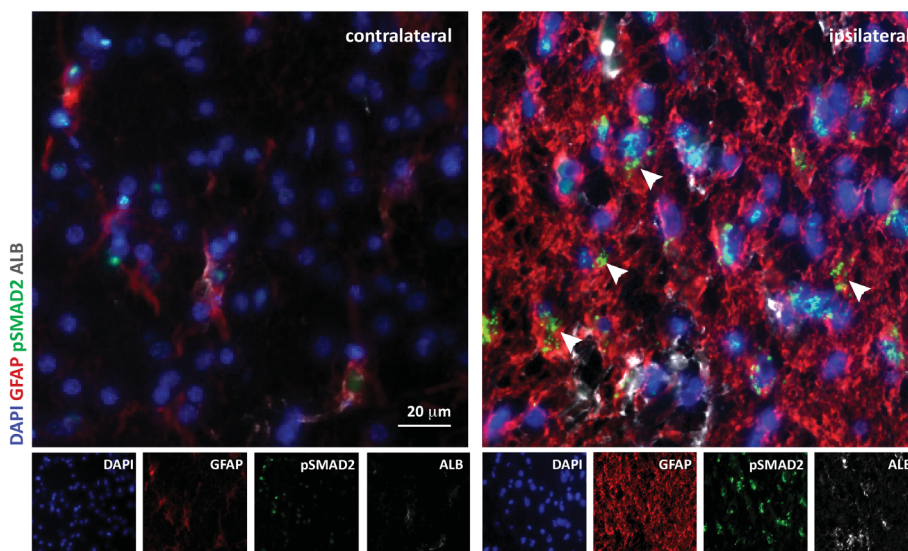


FIGURE 7 Increased expression of transforming growth factor beta (TGF- β) pathway components and inflammation in necrotizing leukoencephalitis. Microscope images of coronal sections of normal contralateral and glial fibrillary acidic protein (BBBD)-affected ipsilateral regions stained for albumin (red), astrocytic marker glial fibrillary acidic protein (GFAP; green), pSmad2 (gray), and DAPI nuclear staining (blue). Increased albumin uptake and pSmad2 expression are colocalized with astrocytes in the brain region where BBBD was detected using dynamic contrast enhancement (DCE) protocol and analysis. Scale bars = 20 μm



The BBB score cutoff of 0.02% yielded a sensitivity of 100%, whereas a cutoff of 6.26% yielded a specificity of 100%. Using this cutoff, seizures were more prevalent in dogs with BBBD compared to dogs with NBBB (72% and 19% for BBBD and NBBB, respectively; $P = .01$, Fisher's exact test).

Total protein concentration in the CSF was available in 29 of the dogs in our study and was not higher in BBBD dogs when compared to dogs with normal BBB (median of 41.4, [range, 9.80-802.73] vs 46.99 [range, 18.50-241.86]; $P > .1$, Mann-Whitney test). Similarly, total nucleated cell count was not significantly higher in BBBD dogs (median of 100 [range, 0-1280] vs 53 [range, 0-300]; $P > .1$, Mann-Whitney test).

4 | DISCUSSION

We present 2 advanced imaging analysis methods for semiquantification of BBB dysfunction in dogs with MUO. We further show that brain regions where BBB leakage was identified by either of these imaging methods indicated higher albumin signal around blood vessels, reactive astrocytes, abundance of microglia, and TGF- β signaling. These cellular and molecular changes were identified using immunofluorescent staining of brain specimens from dogs that were diagnosed with MUO and died from the disease. Only 50% of the MUO dogs in our study were identified with a BBB score above that of the control dogs and hence were defined as BBBD dogs. This proportion is less than could be expected given the inflammatory nature of the disease. The threshold set to determine BBBD could have been high and, therefore, some dogs with BBBD were not detected as such. Using these thresholds, both image analysis methods were sensitive enough to identify brain areas with positive voxels in which contrast agent accumulated. The same brain areas later were identified with BBB leakage using immunofluorescence staining by evidence of albumin extravasation and high signal of the TGF- β downstream protein, pSMAD2. Furthermore, albumin was colocalized with reactive astrocytes and microglia.

The DCE-MRI modality for BBB quantification has been used for more than a decade in humans, experimental animals, and, more recently, in dogs.¹⁸⁻²³ Moreover, methods using quantitative BBBD imaging were shown to be valid in the identification of disease progression in humans.²⁵ However, although repeating the MRI study throughout the course of the disease is possible in dogs, it is the practical aspects that make it uncommonly or rarely performed.

Furthermore, a major limitation of DCE-MRI is the complex imaging requirements, which include initiation of the dynamic sequence before IV contrast injection, followed by repeated scanning. These requirements result in lower spatial resolution and prolongation of anesthesia time, especially in dogs. The DCE-MRI analysis detects the accumulation of contrast material in the tissue over time, indicating BBBD.¹⁸⁻²⁰ Applying our algorithm to this MRI modality, we and others were able to detect areas of BBBD in a subgroup of patients presented with a variety of neurodegenerative and neuropathological disorders, including MUO.¹⁸⁻²⁰

By comparison, the pre-post SEA is a less demanding semiquantitative method in which the mean percentage of contrast-enhanced voxels is used to calculate the BBBD score.^{19,20} In this method, the postcontrast images are taken within minutes after the IV injection of contrast medium. Thus, the rapid passage of tracer in the arterial phase, which occurs within seconds of the injection, is overlooked. This first bolus pass of contrast agent is important mainly for assessment of cerebral blood flow. However, the fraction of contrast material that lingers in the tissue may provide better evaluation of BBB integrity.²³

In our study, the SEA threshold for the determination of permeable voxels was set as the mean PID of the temporal muscle plus 1 SD. Using the same threshold in control dogs, we identified a mean of 0.33% permeable voxels in normal brain. Therefore, MUO dogs were considered with pathological BBBD only if the percentage of positive voxels exceeded 0.33% of total brain parenchyma voxels. This threshold enabled the distinction between MUO dogs with and without seizures. Choosing a lower PID threshold for the determination of permeable voxels potentially would increase sensitivity but decrease specificity of the method in identifying MUO dogs with seizures. Using a threshold that is much higher than the mean PID plus 1 SD of the temporal muscle may miss these subtle changes and identify only brain regions with hypervascularization or severe vascular damage.

All dogs in our study underwent general anesthesia, which was maintained with 1% to 2% isoflurane. A similar anesthesia protocol previously was reported to possibly affect BBB integrity in a cohort of cats in experimental settings.²⁶ In our study, both MUO and control dogs were anesthetized using the same protocol, hence the possible effect of isoflurane on BBB permeability would be redundant in the quantification step.

Meningoencephalitis of unknown origin is a group of inflammatory brain disorders in which the cause of the inflammation is not identified.^{3,7,27} Some patients may display severe, fulminating inflammation with high CSF cellularity and total protein concentration, whereas others exhibit mild clinical signs and clinicopathological findings.^{3,7,27} The identification of intraparenchymal lesions on MRI helps in establishing the diagnosis of MUO in many cases. We showed that using SEA in addition to routine MRI sequences increased the portion of dogs with identified lesions from 50% to 70%. This promising result supports adding pre-post SEA to the routine MRI sequences to increase the sensitivity of MRI in the detection of brain abnormalities in dogs with MUO. Our findings are in agreement with a previous study, which reported higher sensitivity of SEA, as compared to visual evaluation of pre- and postgadolinium images, for the detection of neuroinflammatory conditions.⁷ The increased sensitivity of the SEA method was attributed to the leaky BBB. This notion is supported by our findings of significantly higher AQ in the CSF of MUO dogs with BBBD when compared to MUO dogs with NBBB. Five dogs in our study had lesions that were identified by routine T2 and FLAIR but were not detected by our algorithms. Both described MRI analysis methods are based on the enhancement of contrast agent in the tissue. Therefore, regions with only edema may be missed. One dog with

mild T1 post-contrast enhancement was not identified by SEA because of the high threshold used to increase specificity.

In our study, immunofluorescent staining of brain regions of dogs with MUO where dysfunctional BBB was identified using DCE-MRI or SEA had higher expression of microglia and astrocyte markers, extravasation of albumin, and increased pSMAD expression, supporting the coexistence of BBBD and neuroinflammation in these regions. These findings further support the involvement of TGF- β signaling in the neuroinflammatory cascade in regions where the BBB is disrupted.

Little is known about epileptogenesis in MUO dogs. Activation of TGF- β , followed by increased intracellular pSMAD2, was described in experimental animals as part of a critical modulatory pathway in the astrocytic response to serum albumin, which facilitates the development of epilepsy.^{16,28,29} Furthermore, this pathway was used as a target for epilepsy prevention in animal models.^{16,28,29} Our results support the possibility that this pathway may be associated with epileptogenesis in dogs with MUO as well. Because of the small number of cases available for immunofluorescent evaluation in our study and the lack of fresh brain specimens for biochemical investigation of the described cascade, definitive conclusions could not be drawn. Further investigation of the cellular and molecular mechanisms responsible for seizure development in approximately 20% of dogs with MUO is needed.

In conclusion, the advanced image analysis methods used in our study can serve both clinicians and researchers for the characterization and quantification of BBBD in naturally occurring neurological diseases. Each method has its advantages and limitations, but both were shown to add essential information that enabled the identification of MUO patients with seizures and improved the identification of brain pathology on MRI. When the role of BBBD in the pathogenesis of CNS diseases in dogs is better established, this additional tool will help identify the BBBD as a future target for treatment.

ACKNOWLEDGMENT

The study was funded by the Israeli Science Foundation (ISF) grant number 717-15.

CONFLICT OF INTEREST DECLARATION

Authors declare no conflict of interest.

OFF-LABEL ANTIMICROBIAL DECLARATION

Authors declare no off-label use of antimicrobials.

INSTITUTIONAL ANIMAL CARE AND USE COMMITTEE (IACUC) OR OTHER APPROVAL DECLARATION

The addition of the dynamic sequences was approved by the Hebrew University Veterinary Teaching Hospital Ethics Committee (KSVM-VTH/26_2016) and the owners signed a consent form.

HUMAN ETHICS APPROVAL DECLARATION

Authors declare human ethics approval was not needed for this study.

ORCID

Erez Hanael  <https://orcid.org/0000-0003-1284-895X>

Marco Ruggeri  <https://orcid.org/0000-0002-0150-8178>

Merav H. Shamir  <https://orcid.org/0000-0002-4698-5373>

REFERENCES

1. Talarico LR, Schatzberg SJ. Idiopathic granulomatous and necrotising inflammatory disorders of the canine central nervous system: a review and future perspectives. *J Small Anim Pract.* 2010;51(3):138-149.
2. Wanamaker MW, Vernau KM, Taylor SL, Cissell DD, Abdelhafez YG, Zwingerberger AL. Classification of neoplastic and inflammatory brain disease using MRI texture analysis in 119 dogs. *Vet Radiol Ultrasound.* 2021;62(4):445-454.
3. Cornelis I, Van Ham L, Gielen I, De Decker S, Bhatti SFM. Clinical presentation, diagnostic findings, prognostic factors, treatment and outcome in dogs with meningoencephalomyelitis of unknown origin: a review. *Vet J.* 2019;244:37-44.
4. Hecht S, Adams WH. MRI of brain disease in veterinary patients part 2: acquired brain disorders. *Vet Clin North Am Small Anim Pract.* 2010;40(1):39-63.
5. Granger N, Smith PM, Jeffery ND. Clinical findings and treatment of non-infectious meningoencephalomyelitis in dogs: a systematic review of 457 published cases from 1962 to 2008. *Vet J.* 2010;184(3):290-297.
6. Paušová TK, Tomek A, Šrenk P, Belašková S. Clinical presentation, diagnostic findings, and long-term survival time in 182 dogs with meningoencephalitis of unknown origin from Central Europe that were administered glucocorticosteroid monotherapy. *Top Companion Anim Med.* 2021;44:100539.
7. Dirrig H, Lamb CR. Magnetic resonance imaging of intracranial inflammatory conditions in dogs: sensitivity of subtraction of images versus pre- and post gadolinium T1 weighted image pairs. *Vet Radiol Ultrasound.* 2016;57(4):410-416.
8. Kaczmarek A, José-López R, Czopowicz M, et al. Postencephalitic epilepsy in dogs with meningoencephalitis of unknown origin: clinical features, risk factors, and long-term outcome. *J Vet Intern Med.* 2020;34(2):808-820.
9. Abbott NJ, Friedman A. Overview and introduction: the blood-brain barrier in health and disease. *Epilepsia.* 2012;53(Suppl 6):1-6.
10. Varatharaj A, Galea I. The blood-brain barrier in systemic inflammation. *Brain Behav Immun.* 2017;60:1-12.
11. Varatharaj A, Liljeroth M, Cramer S, et al. Systemic inflammation and blood-brain barrier abnormality in relapsing-remitting multiple sclerosis. *Lancet.* 2017;389:S96.
12. Zenaro E, Piacentino G, Constantin G. The blood-brain barrier in Alzheimer's disease. *Neurobiol Dis.* 2017;107:41-56.
13. Tagge CA, Fisher AM, Minaeva OV, et al. Concussion, microvascular injury, and early tauopathy in young athletes after impact head injury and an impact concussion mouse model. *Brain.* 2018;141(2):422-458.
14. Sweeney MD, Zhao Z, Montagne A, Nelson AR, Zlokovic BV. Blood-brain barrier: from physiology to disease and back. *Physiol Rev.* 2019;99(1):21-78.
15. Friedman A, Kaufer D, Heinemann U. Blood-brain barrier breakdown-inducing astrocytic transformation: novel targets for the prevention of epilepsy. *Epilepsy Res.* 2009;85(2-3):142-149.
16. Weissberg I, Wood L, Kamintsky L, et al. Albumin induces excitatory synaptogenesis through astrocytic TGF- β /ALK5 signaling in a model of acquired epilepsy following blood-brain barrier dysfunction. *Neurobiol Dis.* 2015;78:115-125.
17. Salar S, Lapilover E, Müller J, et al. Synaptic plasticity in area CA1 of rat hippocampal slices following intraventricular application of albumin. *Neurobiol Dis.* 2016;91:155-165.

18. Hanael E, Veksler R, Friedman A, et al. Blood-brain barrier dysfunction in canine epileptic seizures detected by dynamic contrast-enhanced magnetic resonance imaging. *Epilepsia*. 2019;60(5):1005-1016.
19. Bar-Klein G, Lublinsky S, Kamintsky L, et al. Imaging blood-brain barrier dysfunction as a biomarker for epileptogenesis. *Brain*. 2017;140(6):1692-1705.
20. van Vliet EA, Otte WM, Wadman WJ, et al. Blood-brain barrier leakage after status epilepticus in rapamycin-treated rats I: magnetic resonance imaging. *Epilepsia*. 2016;57(1):59-69.
21. Veksler R, Shelef I, Friedman A. Blood-brain barrier imaging in human neuropathologies. *Arch Med Res*. 2014;45(8):646-652.
22. Weissberg I, Veksler R, Kamintsky L, et al. Imaging blood-brain barrier dysfunction in football players. *JAMA Neurol*. 2014;71(11):1453-1455.
23. Chassidim Y, Veksler R, Lublinsky S, Pell GS, Friedman A, Shelef I. Quantitative imaging assessment of blood-brain barrier permeability in humans. *Fluids Barriers CNS*. 2013;10(1):9.
24. Goksuluk D, Korkmaz S, Zararsiz G, Ergun Karaagaoglu A. easyROC: an interactive web-tool for ROC curve analysis using R language environment. *R J*. 2016;8(2):213.
25. Lublinsky S, Major S, Kola V, et al. Early blood-brain barrier dysfunction predicts neurological outcome following aneurysmal subarachnoid hemorrhage. *EBioMedicine*. 2019;43:460-472.
26. Tétrault S, Chever O, Sik A, Amzica F. Opening of the blood-brain barrier during isoflurane anaesthesia. *Eur J Neurosci*. 2008;28(7):1330-1341.
27. Coates JR, Jeffery ND. Perspectives on meningoencephalomyelitis of unknown origin. *Vet Clin North Am Small Anim Pract*. 2014;44(6):1157-1185.
28. Kim SY, Senatorov VV, Morrissey CS, et al. TGF β signaling is associated with changes in inflammatory gene expression and perineuronal net degradation around inhibitory neurons following various neurological insults. *Sci Rep*. 2017;7(1):7711.
29. Bar-Klein G, Cacheaux LP, Kamintsky L, et al. Losartan prevents acquired epilepsy via TGF- β signaling suppression. *Ann Neurol*. 2014;75(6):864-875.

SUPPORTING INFORMATION

Additional supporting information may be found in the online version of the article at the publisher's website.

How to cite this article: Hanael E, Baruch S, Chai O, et al. Detection of blood-brain barrier dysfunction using advanced imaging methods to predict seizures in dogs with meningoencephalitis of unknown origin. *J Vet Intern Med*. 2022;36(2):702-712. doi:10.1111/jvim.16396